

Improved structure for SOI diode uncooled infrared focal plane arrays

JIANG Wen-Jing*, OU Wen, MING An-Jie, LIU Zhan-Feng, YUAN Feng

(Key Laboratory of Microelectronics Devices & Integrated Technology
Institute of Microelectronics of Chinese Academy of Sciences, Beijing 100029, China)

Abstract: The silicon-on-insulator(SOI) diode uncooled infrared focal plane array(IR FPA) uses single-crystal silicon PN junction diodes as a temperature sensor, and has various advantages over other MEMS-based uncooled IR FPAs. The basic principle and the advances of the two different SOI diode uncooled IR FPA are describes, including operation of the diode temperature sensor, the design of the pixel structure, the theory calculation and the simulation results. The improved structure, the IR absorbing structure was made in the upper level to cover almost the entire pixel area, in which the fill factor can increase from 21% to 80%. The calculated results show that the sensitivity of the improved structure raises to $7.75 \times 10^{-3} \text{V/K}$ and the noise equivalent temperature difference(NETD) decreases to 43 mK ($f/1.0$) in a $35 \mu\text{m} \times 35 \mu\text{m}$ micromachined structure, which is close to the international advanced level. Meanwhile, the simulation results also confirm the improved performance and the possibility for large format uncooled IR FPAs.

Key words: SOI, diode, fill-factor, infrared focal plane arrays(IR FPA)

PACS: 87.80. Ek, 87.64. km

SOI 二极管型非制冷红外焦平面结构的改进设计

蒋文静*, 欧文, 明安杰, 刘战锋, 袁峰

(中国科学院微电子所, 器件与集成技术重点实验室, 北京 100029)

摘要: 在绝缘衬底上的硅(SOI)制备的二极管型非制冷红外焦平面是利用单晶硅PN结二极管作为温度探测器, 比其它类型非制冷红外焦平面具有自己的独特优势. 描述了传统型像素的结构与特性, 并提出一种改进型结构. 在传统的像素结构中, 红外吸收结构直接覆盖于二极管表面, 其填充系数仅为21%. 改进后的结构将红外吸收层悬空并覆盖整个像素表面, 使吸收结构能够达到80%, 大大提高了器件的吸收率. 计算结果也显示改进后的结构在像素尺寸为 $35 \mu\text{m} \times 35 \mu\text{m}$ 时, 器件的灵敏度可达到 $7.75 \times 10^{-3} \text{V/K}$, 等效功率噪声(NETD)可减小至43 mK($f/10.0$). 同时, ANSYS的仿真结果也表明改进后的结构在吸收率上的提高, 证明了此结构的可行性.

关键词: 绝缘衬底上的硅; 二极管; 填充系数; 红外焦平面

中图分类号: TN4 **文献标识码:** A

Introduction

Recently uncooled infrared(IR) imaging technology has been widely applied to such fields as surveillance, biomedical diagnostics, intelligence agriculture and auxiliary safety systems for moving bodies. Since uncooled IR focal plane arrays(FPAs) do not need cryogenic coolers, uncooled IR cameras are much superior in size, cost and

lifetime and power consumption compared with cooled IR cameras. Although many approaches have been proposed for uncooled IR FPAs, most of them use materials for the temperature sensing element, which are not commonly used in Si-LSI(Large Scale Integration) process. For the SOI diode uncooled IR FPA, single-crystal silicon PN junction diodes are used as a temperature sensor, which is not only commonly used in Si-LSI process, but also promises high uniform responsivity and productivity. And

Received date: 2013-01-04, **revised date:** 2013-03-21

收稿日期: 2013-01-04, **修回日期:** 2013-03-21

Foundation items: Project supported by the Beijing Science and Technology Project(Z111104055311062), and Key Laboratory of Microelectronics Devices & Integrated Technology.

Biography: Jiang Wen-Jing(1983-), female, Beijing, doctor. Research area involves Micro-Electro-Mechanical Systems with infrared imaging system. E-mail: jiangwenjing@ime.ac.cn

* **Corresponding author:** E-mail: jiangwenjing@ime.ac.cn

it has already been applied in practice^[1-3].

The SOI diode uncooled IR FPAs are expected to play an inimitable role in the commercialization of infrared imaging technology. In the conventional design, absorbing area only covers the PN junction diodes, caused low fill factor^[2]. Since the fill factor is defined as ratio of detection area to the detector area; its values depend on the structure design and the shape of the supporting leg. Compared with our conventional design, in order to further reduce the pixel size and to improve device performance, a high fill-factor structure is proposed.

The basic principle and the advances of the improved SOI diode uncooled IR FPA are discussed in this paper, including operation of the diode temperature sensor, the design of the pixel structure, the theory calculation and the simulation results. Finally analysis shows that the device performance has been sharply improved by our new design with high fill factor.

1 Theory of diode temperature sensor

As we know electrical characteristics of the PN junction is sensitive to temperature, which can be used for temperature sensing in uncooled IR FPAs. An ideal diffusion-limited characteristic of a diode function with the forward-bias voltage V_f and the current I_f is given by

$$I_f = S_d \cdot J_s \cdot \exp(-qV_f/kT) \quad , \quad (1)$$

where S_d is the junction area, J_s is the saturation current, q the magnitude of electronic charge, k the Boltzmann's constant, T the temperature.

Figure 1 shows voltage-current characteristics of a diode at two different temperatures, the forward voltage of a PN junction decreases with the increasing temperature. The typical data, which means the variance of forward voltage with temperature changes 1 °C, of the silicon PN junction is 2 mV/°C^[4], and this is the basic theory for our uncooled IR FPAs.

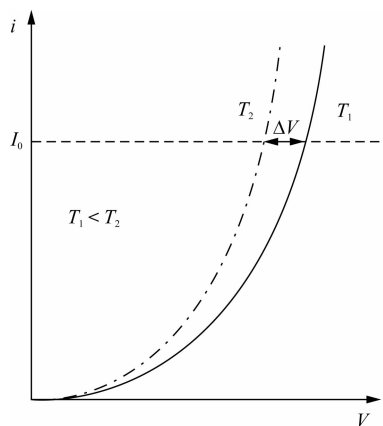


Fig. 1 Operation of the diode temperature sensor
图1 二极管温度探测器原理图

2 SOI-diode detector pixel design

Conventional design (Type 1) of the SOI diode uncooled IR FPAs is shown in Fig. 2: the PN junction diodes formed in a suspended plate are used as a temperature sensor, and the plate is supported by two thermal in-

terconnects with electrical interconnections, the IR absorber is directly fabricated on the PN junction diodes, and filled with the dielectric film with a thickness of 1/4 wavelength of IR radiation^[4-5]. Type 1 design has a simple fabrication process, but the IR absorbing area is limited and equal to the temperature sensor, this result in a fill factor 20% only.

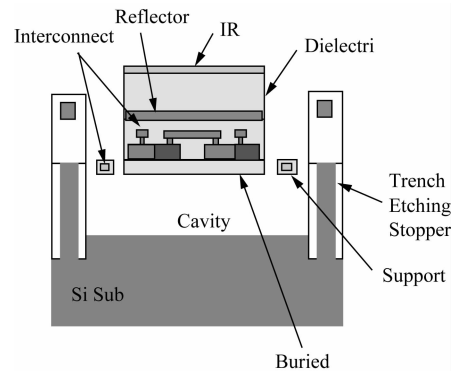


Fig. 2 The cross sectional pixel structure for conventional structure (Type 1)

图2 传统结构的剖面图(结构1)

To obtain higher sensitivity, the thermal conductance of the support leg is designed to be as small as possible and the infrared-absorbing area is designed to be as big as possible. So a novel design with fill factor of 80% has been proposed. Figure 3 shows a cross section of a pixel structure of improved design (Type 2), the dielectric film has been replaced by a vacuum gap with the same thickness, and the IR absorber is supported by two thin pillars. Thus the IR absorbing area forward voltage is expanded to the whole pixel, consequently, the fill factor is increased to 80%.

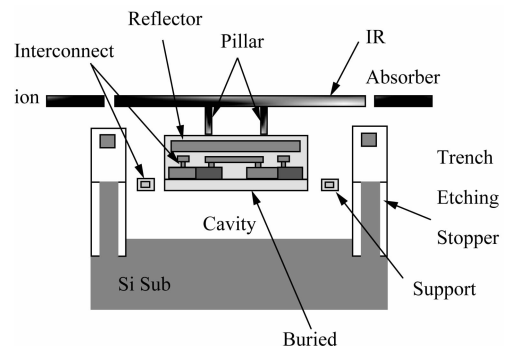


Fig. 3 The cross section of a pixel structure of the improved design (Type 2)

图3 改进型像素结构的剖面图(结构2)

3 Performance estimation

Prediction for the performance in vacuum is obtained using simple analytical expressions for thermal conductance, the thermal time constant, the sensitivity and the noise equivalent temperature difference (NETD).

The device performance can be estimated by the thermal conductance, the thermal time constant, the sensitivity and the noise equivalent temperature difference (NETD).

The thermal conductance is given by^[6-7]:

$$G = G_r + G_{log} = 4A\varepsilon\Delta T^3 + \sum_i \frac{\lambda_i w_i d_i}{l_i},$$

where A is the area of the detector, ε the emissivity, σ the Stefan constant, T the temperature of the detector, λ_i , w_i , d_i , l_i is the thermal conductivity, width, thickness, length for different film, respectively.

The thermal time constant:

$$\tau = C/G,$$

where C is the total thermal capacity.

The output voltage is given by:

$$V_s = n \frac{dV}{dT} \Big|_s \Delta T,$$

where n is the number of the PN junction, $\frac{dV}{dT} \Big|_s$ is the temperature sensitivity of a PN junction, ΔT is the temperature difference.

The sensitivity is given by:

$$R_v = V_s/q,$$

where q is the power of radiation.

The NETD is given by:

$$\delta T_s = \frac{V_n}{n \frac{dV}{dT} H},$$

where V_n is the total noise voltage, H is the ratio between the temperature difference of the detector and the temperature difference of the objective.

Assuming the incidence radiation heat flux density is 200 W/m^2 , the environment temperature is 300 K , the absorption coefficient is 1, and the size of those two structures is $35 \times 35 \text{ }\mu\text{m}$. The comparison in Table 1 shows that, performance of type 2 device has been obviously improved. The sensitivity of the Type 2 structure increased from $1.37 \times 10^{-4} \text{ V/K}$ to $7.75 \times 10^{-3} \text{ V/K}$, which is almost double that of Type 1 structure. The NETD decreased from 126 mK to 42 mK . Meanwhile, the thermal time constant is little more than that of Type 1 structure, since the disappeared dielectric lowered the thermal conductance, but it still is acceptable for practical application.

Table 1 Calculated performance

表 1 性能的计算结果

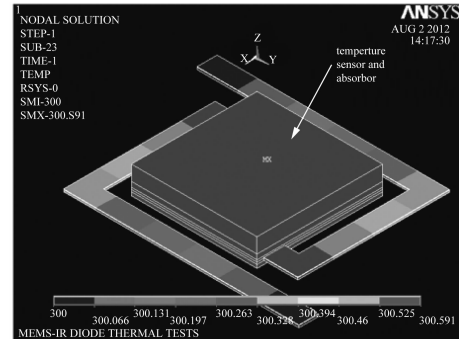
Performance	Type 1	Type 2
Thermal conductance(W/K)	9.2×10^{-8}	6.19×10^{-8}
τ_{th} (msec)	17.8	21.9
Sensitivity(V/K)	1.37×10^{-4}	7.75×10^{-3}
NETD(@f/1.0)(mK)	126	42

4 Thermal modeling

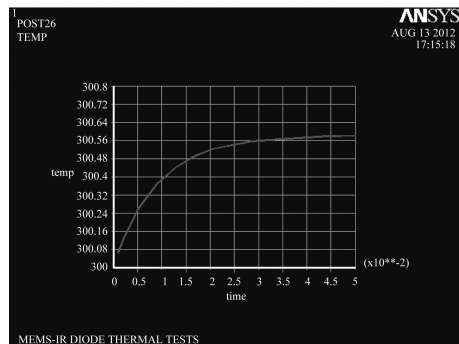
In this work the heat transfer within the detector has been solved by using the computational fluid dynamics (CFD) model^[8]. An ANSYS model has been used to solve and predict the behavior of the heat transfer for the PN junction diodes.

Finite element analysis(FEA) simulations were performed for the design with the same parameters as that adopted in the theoretical calculation. Temperature distri-

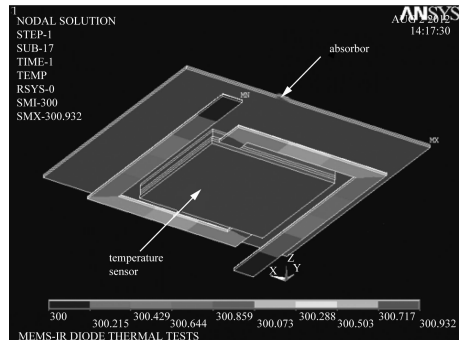
bution for different structure is shown in Fig. 4(a) and (c), and the relationship between the temperature and the thermal time is shown in Fig. 4(b) and(d).



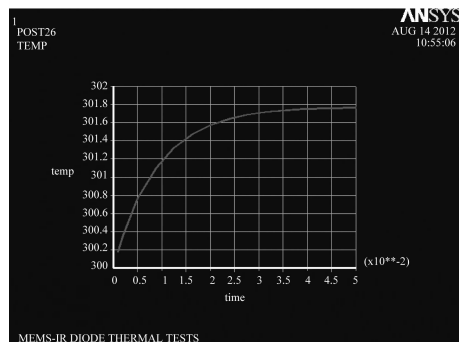
(a)



(b)



(c)



(d)

Fig. 4 (a) Nodal temperature distribution for Type 1; (b) the relationship between the temperature and the thermal time for Type 1; (c) Nodal temperature distribution for Type 2; (d) the relationship between the temperature and the thermal time for Type 2

图 4. (a) 结构 1 的温度分布图; (b) 结构 1 温度与热响应时间的关系曲线; (c) 结构 2 的温度分布图; (d) 结构 2 温度与热响应时间的关系曲线

From the simulation results, it is clear that with the same incidence radiation heat flux density, the temperature of the sensor will increase 0.591 °C and 1.932 °C for Type 1 and Type 2 structure, respectively. It means that the output voltage is much higher than before, so the sensitivity of the device enhances correspondingly. The thermal time constants of the two structures is 27 ms and 33 ms, respectively, since the vacuum condition is not taken into account in the simulation, the thermal time constant is higher than the calculated value. All of these demonstrate the feasibility of the Type 2 structure.

5 Conclusion

The improved structure with the absorbing structure suspending above the PN junction diodes and covering almost the entire pixel area, dramatically increases fill factor from 21% to 80%. Both the simulation and theoretical calculation demonstrated that the performance of the SOI diode uncooled IR FPAs is much improved in performance.

References

- [1] Ishikawa T, Ueno M, Endo K, *et al.* Low-cost 320 × 240 uncooled IRFPA using a conventional silicon IC process [J]. *Proc. SPIE*, 1999, 3689, 556 – 564.
- [2] Kosasayama Y, Sugino T, Ohta Y, *et al.* Pixel scaling for SOI-diode uncooled infrared focal plane arrays [J]. *Proc. SPIE*, 2004, 5406, 504 – 511.
- [3] Li C, Han C J, Skidmore G D, *et al.* DRS uncooled VOx infrared detector development and production status [J]. *Proc. SPIE*, 2010, Vol. 7660, 76600V.
- [4] Miller R G J, Stace B C. The experimental method of infrared spectroscopy [M]. *CHINA MACHINE PRESS*, 1985, 66 – 68.
- [5] Popova S I, Tolstych T S, Vorob'ev V T. Optical characteristics of amorphous SiO₂ in the region 1400-200 cm⁻¹ [J]. *Optika Spektrose*, 1972, 33, 801 – 803.
- [6] Biao Li. Design and simulation of an uncooled double-cantilever microbolometer with the potential for ~ mK NETD [J]. *Sensors and Actuators A*, 2004, 112, 351 – 359.
- [7] Kruse P W. *Uncooled Thermal Imaging, Arrays Systems and Applications* [M]. SPIE Press, 2001, Bellingham, WA.
- [8] Selim Eminoglu, Deniz Sabuncuoglu Tezcan, Yusuf Tanrikulu M, *et al.* Low-cost uncooled infrared detectors in CMOS process [J]. *Sensors and Actuators A*, 2003, 109, 102 – 113.